Optics & Laser Technology 167 (2023) 109798

Contents lists available at ScienceDirect

Optics and Laser Technology

journal homepage: www.elsevier.com/locate/optlastec

Full length article

Doughnut beam shaping based on a 3D nanoprinted microlens on fiber tip

Zhuorong Li [a,b,1], Bozhe Li [a,b,1], Dejun Liu [a,b,*], Liqing Jing [a,b], Jiaqi Wang [a,b], Cailing Fu [a,b], Yiping Wang [a,b], Changrui Liao [a,b]

[a] Shenzhen Key Laboratory of Photonic Devices and Sensing Systems for Internet of Things, Guangdong and Hong Kong Joint Research Centre for Optical Fibre Sensors, State Key Laboratory of Radio Frequency Heterogeneous Integration, Shenzhen University, Shenzhen 518060, China

[b] Shenzhen Key Laboratory of Ultrafast Laser Micro/Nano Manufacturing, Key Laboratory of Optoelectronic Devices and Systems of Ministry of Education/Guangdong Province, College of Physics and Optoelectronic Engineering, Shenzhen University, Shenzhen 518060, China

ARTICLE INFO

Keywords:
Optical Fiber
Femtosecond laser
3D Printing
Beam shaping
Microlens

ABSTRACT

Spatial beam intensity shaping is of great significance in many applications, such as laser fabrication and medical treatment. In this study we present a new method for doughnut beam shaping based on 3D nanoprinted microlens on fiber tip. The optical structure of the microlens was first designed and optimized based on illumination optics in software, and then the microlens was fabricated on a single-mode-fiber tip by femtosecond laser induced two-photon polymerization. Both simulation and experiment results have demonstrated that the Gaussian beam output from a single-mode fiber can be successfully transferred to a high-quality doughnut beam by using the fiber-tip microlens. The proposed microlens shows larger tolerance in fabrication resolution compared with optical diffraction beam shaping elements. Our research shows that the femtosecond laser induced two-photon polymerization provides a new and flexible method for the integration of micro-scaled beam shaping elements on optical fibers.

1. Introduction

High quality micro-optical elements have been attracting growing attentions in various applications, such as illumination, fiber endoscopes [1] and compound-eye camera [2]. A number of micromachining technologies have been applied for fabrication of micro-optical elements, for example ultra-precision broaching [3], diamond turning [4], ink-jet printing [5], and so on. Individual micro-optical elements can be well manufactured using the above technologies, however the assembling of multiple micro-optical elements is difficult, a small central misalignment between different elements may lead to significant reduction in light beam quality.

Femtosecond laser induced two-photon polymerization (TPP) allows for the fabrication of micro-optical elements with feature sizes below 100 nm [6]. Thus, it has been extensively investigated in field of integrated micro optics. High-quality cascaded micro-optical elements can be directly and accurately nanoprinted on the surface of various substrates, such as on the end face of an optical fiber [7–12], a CMOS surface [13], and a LED surface [14], and the whole process avoids the problem of precision assembly. Micro-optical elements can be used to precisely regulate the propagation properties of the light beam, such as polarization states and intensity distribution. In recent years, TPP has been widely used for fabrication of highly integrated micro-optical elements, for example diffractive optical element [11], hybrid refractive–diffractive optical component [12,15], photonic crystal [16], free-form surface refractive lens [10], multi-lens objective [17]. The 3D nanoprinted micro-optical elements have been successfully applied in the field of optical coherence tomography (OCT) endoscope [18], and fluorescence measurement [19] and may find more applications in photothermal therapy [20].

Fiber-tip microlens utilizes the advantages of compact size and flexibility of an optical fiber, it can go deep into tiny holes or hollow organs where other devices cannot approach. It provides possibilities for getting internal information of some narrow spaces, such as blood vessels [18,19]. Usually the fiber-tip microlens performs three types of functions, i.e. focusing, imaging and beam shaping. Beam shaping for optical fibers is important in medical treatment and laser fabrication and it can be achieved by the use of diffractive optical element (DOE) or refractive microlens with free-form surface. In some cases, for example trapping of atoms, optical tweezers, and in the lighting system of

* Corresponding author.
E-mail address: dejun.liu@szu.edu.cn (D. Liu).

[1] These authors contributed equally to this works: Zhuorong Li, Bozhe Li.

https://doi.org/10.1016/j.optlastec.2023.109798
Received 4 May 2023; Received in revised form 12 June 2023; Accepted 3 July 2023

lithography and laser welding, it is required to change the Gaussian intensity distribution into a doughnut shaped intensity distribution [21–23]. However, the traditional beam-shaping elements suffer from large size and assembling issues. Recently, Gissibl et al. designed and successfully fabricated a microsized phase masks on fiber tip by femtosecond direct laser writing for spatial beam intensity shaping [11], however such diffraction elements raised an ultra-high fabrication resolution for the equipment of less than 10 nm. In this letter, we propose a more accessible on-fiber microlens designed based on illumination optics. The microlens with free-form surface was nanoprinted on the end face of a single-mode fiber (SMF) by a TPP method. The printing resolution of TPP used in our experiment in X, Y and Z direction can reach up to 100 nm, 100 nm and 300 nm, and the root-mean-square (RMS) error of the free-form surface between design and measurement is 289 nm. With the help of this microlens the Gaussian beam output from the fiber end is successfully shaped into a high-quality Doughnut beam. A schematic diagram of this doughnut beam generator is illustrated in Fig. 1.

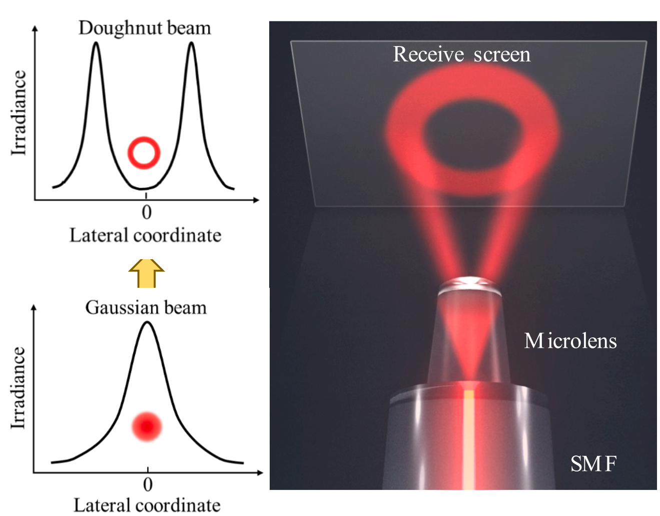

Fig. 1. Schematic diagram of the doughnut beam generator based on a fiber-tip microlens.

2. Optical design

2.1. Source measurement

Beam shaping can be considered as illumination optics. The key factor of the optical design based on illumination optics is the etendue balance of optical system. For a circular planar light source, the etendue can be simplified as [24]:

$$U = \pi \cdot (n \cdot NA)^2 \cdot A \tag{1}$$

where n is the refractive index of the medium, NA is the numerical aperture of light source, A is the area of light source. Note that, only when the source etendue is smaller than that of the system can there be a variable space for optical design without loss of light energy [25]. In this work, a SMF (Corning HI780) with a core diameter of 5 μm and a NA of 0.14 is used. Due to the small etendue of the fiber ($1.2 \times 10^{-12} mm^2 \cdot sr$), it allows for the free design and optimization of physical size of the fiber-tip microlens, so that different types of free-form lenses can be designed and fabricated on the end face of the fiber to shape the output beam.

A 830-nm laser source was launched into the SMF with fundamental mode operation and the light beam output from the fiber was recorded by a commercial near-field luminous intensity measurement system (Radiant Vision Systems, SIG-400), as shown in Fig. 2(a). The SMF was fixed by a fiber clamp that was mounted on a Goniometer Stage. The

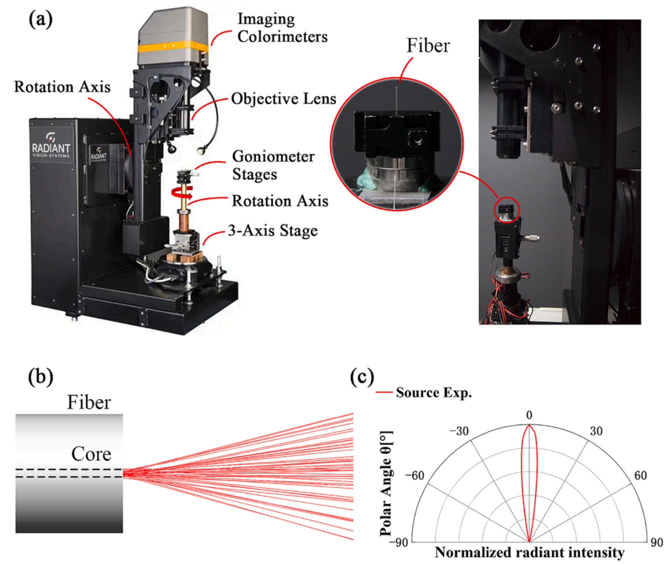

Fig. 2. (a) Near-field luminous intensity measurement system SIG-400. (b) Cross-sectional view of rays emitted from the end face of an SMF. (c) Normalized polar plot of the radiant intensity output from an SMF.

output beam from the SMF was collected by an Imaging Colorimeter with a 20x Objective Lens. A 3-Axis Stage and a Goniometer Stage were used to align the axises of the fiber and Objective Lens. During the test, the beam intensity distribution output from the SMF was measured at different angles by rotating the fiber and the Objective Lens. Fig. 2(b) shows the ray tracing of the beam output from the fiber end face, where the beam spreads within a full-width angle (10% threshold) of 20° along the optical axis. The measured beam intensity distribution of the SMF is illustrated in Fig. 2(c). It can be seen that the light intensity reaches its maximum at 0°, namely the direction of the optical axis, and it gradually falls with the increase of the divergent angle between the light and the optical axis. On the whole, the light intensity presents a Gaussian distribution with the change of spatial angle and the full-width-half-maximum (FWHM) is obtained at 14°. When the spatial angle to the optical axis is greater than 10°, the light intensity reduces to 0.

2.2. Microlens design

Fig. 3 shows the diagrams of the microlens design that is obtained

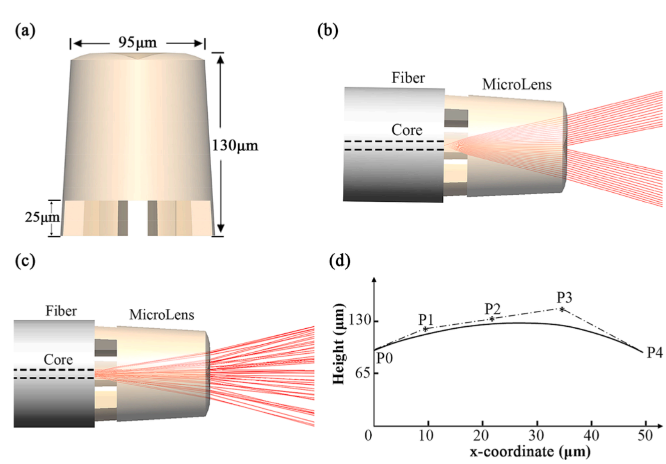

Fig. 3. (a) Geometry parameters of the designed microlens on fiber tip. (b) Ray tracing diagram of an ideal point light source. (c) Ray tracing diagram with the measured fiber-tip light source. (d) Final optimized quartic Bezier curve for formation of free-form surface of microlens.

based on least-squares optimization. As shown in Fig. 3. (a), the microlens has a flat incident face with a diameter of 110 μm and a free-form output face with a diameter of 95 μm and the overall height of the microlens is 130 μm. Because the data of the light source was measured in air, an air gap with a height of 25 μm was additionally designed between the fiber end face and the incident face of microlens to match with the experimental measurement. A binary map of a doughnut shaped pattern with an inner diameter of 2 mm and an outer diameter of 5 mm was imported into simulation software to optimize the microlens design. Of particular note is that the initial microlens structure is very important, since the final structure of microlens is obtained through an iterative loop optimization on the basis of initial structure. If the initial parameters such as the curvature, conic constant, and the coordinates of the curve control points are set improperly, the expected light intensity distribution cannot be obtained. In particular, the geometry parameters of the microlens is obtained and optimized by tracing the geometric rays emitted from a point light source as shown in Fig. 3(b). The 2D output cross sectional surface profile of the microlens is designed based on a quartic Bezier curve because it shows good smoothness and flexibility, it is easy to increase or decrease its control points as needed, and the curvature of the curve is less likely to show sudden variations. A quartic Bezier curve satisfies the following Equation:

$$P(t) = P_0(1-t)^4 + 4P_1(1-t)^2 t + 6P_2(1-t)^2 t^2 + 4P_3(1-t)t^3 + P_4 t^4 \tag{2}$$

where P_0, P_1, P_2, P_3, P_4 are the radial coordinate of the curve control points and t values from 0 to 1. The initial quartic Bezier curve is designed as a straight line. To obtain the intensity distribution of doughnut shape, each geometric light should diverge away from the optical axis, therefore, the coordinates of the control points are gradually optimized based on the simulation results, and eventually a curve profile is obtained. However, the real light source is not an ideal point source. The measured data of the fiber-tip light source was imported into the software to further optimize the structure of microlens, as shown in Fig. 3(c). The final optimized coordinates of the control points of the final surface are P_0= (0,124.95), P_1= (9.14, 128.63), P_2= (21.29, 130.48), P_3= (33.09, 132.28), P_4= (47.69, 124.53) as shown in Fig. 3 (d). The surface profile of the microlens is then obtained by rotating the curve profile along its optical axis. It is found that the light is not as divergent as the point light source due to the extended light source employed. In simulation, the refractive index of the microlens is set to be 1.5037 @ 800 nm [26].

3. Fabrication

The optimized microlens was then fabricated by TPP. To achieve a smooth printing surface and hence good optical performance of the microlens, IP-S purchased from Nanoscribe was used as the photoresist. Coaxiality between the SMF and microlens are significantly important to achieve a systematic intensity distribution of the doughnut beam output. Before fabrication, the SMF was well cleaved and clamped by a customer designed fixture to ensure that the fiber endface was perpendicular to the laser, and then a frustum with the same diameter as that of the fiber was printed to calibrate the laser position. After that the calibrated position was precisely aligned with the fiber with the help of CCD image, and then the fiber was well aligned and ready for printing. The SMF tip was immersed in the photoresist, femtosecond laser pulses with a central wavelength of 780 nm, a pulse width of 100 fs, and a repetition rate of 80 MHz were focused in the photoresist by a 25x oil-immersed objective with a NA of 0.8. The 3D printing was achieved by scanning the laser beam along the X/Y axis and Z axis layer by layer via galvanometric mirrors and a high precision piezo stage, respectively. The optimized laser energy and scanning speed were set as 0.2 nJ and 50 mm/s, respectively. The layer spacing along Z-axis was set as 0.2 μm, and the line spacing in X-Y plane was set as 0.3 μm. The printing resolution of TPP in X, Y and Z direction can reach up to 100 nm, 100 nm and 300 nm, which are mainly dependent on femtosecond laser pulse energy and printing speed. After TPP fabrication, the printed microlens was immersed in propylene glycol methyl ether acetate (PGMEA) for 5 min to remove the unexposed photoresist and subsequently soaked in isopropanol for 3 min to remove the remaining PGMEA. Then the fiber-tip microlens was ready for the following optical characterization.

Fig. 4(a) and (b) show the scanning electron microscope (SEM) images of the microlens observed from different angles of view. It can be seen that the free-form surface and the air gap of microlens are well presented and it has a smooth printing surface. The only deficiency observed is that the bottom supporting structure of microlens is not closely attached with the end face of fiber and this can be explained by the irregular shrinkage and the deformation of photoresist during printing and development process. Fig. 4 (c-d) show the designed and measured free-form surfaces of microlens that is profiled with a white-light interferometer (Atometrics, EX230). The RMS error between design and measurement is calculated to be 289 nm. This error may result from the employed layer-by-layer printing method and the structural shrinkage and deformation during the development. It can be reduced by further optimization of the fabrication parameters such as laser pulse energy, printing speed and scanning spacing.

4. Results and discussion

The normalized beam intensity distribution at a distance of 10 mm from the fiber-tip microlens was simulated and measured by SIG-400 with the corresponding results being compared in Fig. 5(a-b). Both the simulation and experiment demonstrate that the Gaussian beam output from SMF is well redistributed into a high-quality doughnut beam. Fig. 5 (c-d) illustrate the intensity distribution in the cross sections of X = 0 and Y = 0. In the simulation, the light intensity is minimum at the center and it reaches maximum at 1.36 mm away from the center at both cross sections. However, the intensity distribution in the experiment shows a slight asymmetry. The minimum and maximum light intensities in the cross sections of X = 0 appears at 0.085 mm and 1.51 mm, while in the cross sections of Y = 0 the intensity has a minimum and maximum values at −0.17 mm and 1.7 mm away from the center, respectively. The

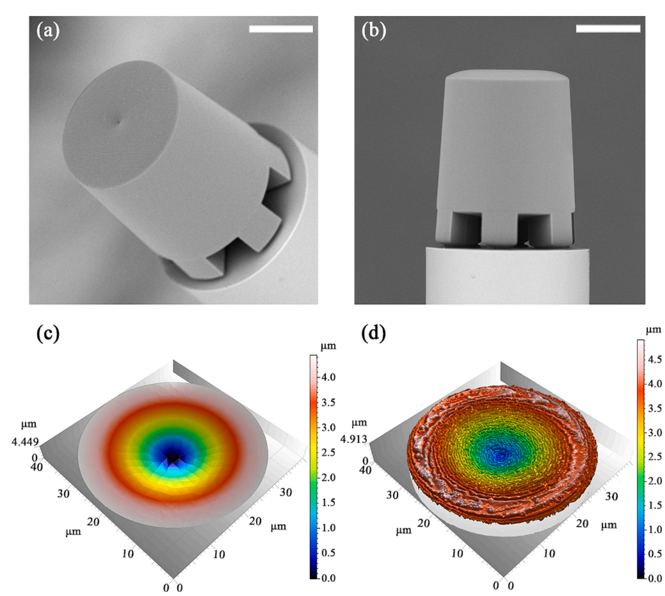

Fig. 4. SEM images of the 3D nanoprinted fiber-tip microlens in (a) top view and (b) side view. (scale bars: 50 μm) (c) Designed free-form surface of microlens. (d) Measured surface topography of the printed microlens by a white-light interferometry.

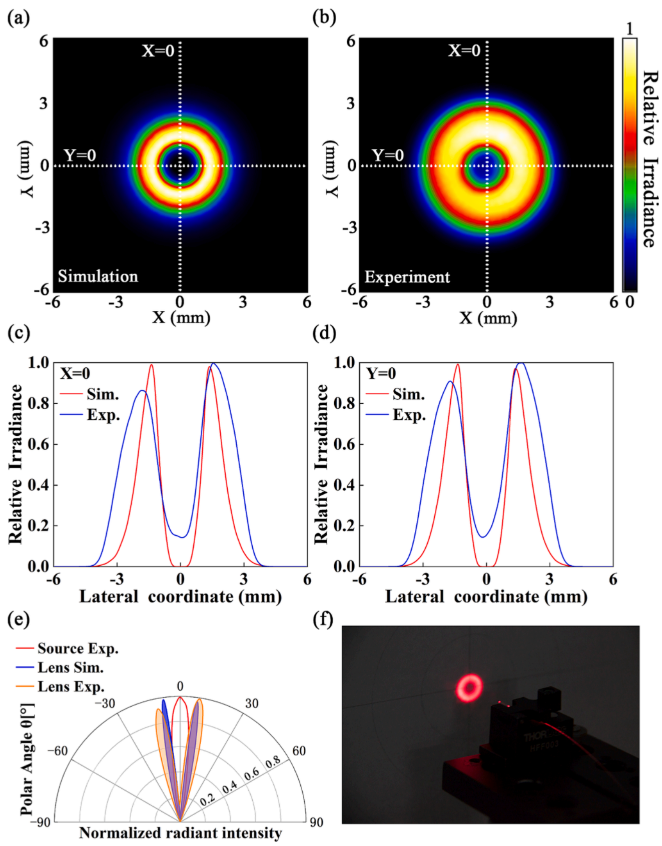

Fig. 5. Normalized light intensity distributions in (a) simulation and (b) experiment. Light intensity distribution at the cross sections of (c) X = 0 and (d) Y = 0. (e) Normalized polar plot of radiant intensity. (f) Doughnut beam recorded on the receiving screen in dark room.

asymmetry of intensity distribution may be explained by the imperfect coaxality among the SMF, microlens and objective lens.

For a better comparison, a polar plot of radiation intensity varying with spatial angle is given in Fig. 5(e). Similarly, it can be seen that the intensity distribution in the optical simulation shows a good symmetry, the minimum and maximum intensities are obtained at 0° and 8°, while in the experiment, the minimum and maximum intensities appears at $-2^{\circ}$and 9°, respectively. The size difference of the doughnut beams between simulation and experiment can be attributed to the surface quality imperfection of the printed microlens. The proposed on-fiber microlens and its beam shaping results are comparable with that of on-fiber diffraction elements but with much more tolerance in fabrication resolution. In order to more intuitively show the beam shaping effect, a red laser (655-nm) was coupled into the SMF and the fiber-tip microlens, it is noted that the SMF is no longer simgle mode transmission at 655 nm, but still a high-quality doughnut beam was observed on the receiving screen in the dark room environment, as shown in Fig. 5(f).

5. Conclusion

In conclusion, we have demonstrated a miniaturized microlens directly printed on the end face of a SMF for doughnut beam shaping. The fiber-tip microlens was printed by TPP with dip-in approach. The RMS error between the designed and printed surface is 289 nm. Both simulation and experiment have demonstrated that such a fiber-tip microlens is able to transfer Gaussian beam to high-quality doughnut beam. It is verified that TPP nanoprinting method has great advantages in the integrated manufacturing of micro-optical elements on fiber tip. It is noted that in this paper we have demonstrate the proof of concept of design and fabrication of beam shaping element on a fiber tip. Fused silica glass has better properties in optical transparency, thermal and chemical resistance than polymer based photoresist. If fused silica glass is used as the photoresist, the beam shaping microlens may find broader applications in optics and photonics such as endoscope, photothermal therapy and fiber laser fabrication.

CRediT authorship contribution statement

Zhuorong Li: Conceptualization, Formal analysis, Methodology, Software, Writing – original draft. **Bozhe Li:** Formal analysis, Investigation, Methodology, Writing – original draft. **Dejun Liu:** Conceptualization, Formal analysis, Methodology, Software, Supervision, Writing – review & editing. **Liqing Jing:** Formal analysis, Software. **Jiaqi Wang:** Formal analysis. **Cailing Fu:** Formal analysis, Writing – review & editing. **Yiping Wang:** Supervision, Resources. **Changrui Liao:** Supervision, Conceptualization, Writing – original draft.

Declaration of Competing Interest

The authors declare that they have no known competing financial interests or personal relationships that could have appeared to influence the work reported in this paper.

Data availability

Data will be made available on request.

Acknowledgements

This work was supported by National Natural Science Foundation of China (62122057, 62075136, 62105217), and the Science and Technology Innovation Commission of Shenzhen (RCYX20200714114524139, JCYJ20190808173401660, JCYJ20200109114001806, JCYJ20200109114020865).

References

[1] B. Li, C. Liao, Z. Cai, J. Zhou, C. Zhao, L. Jing, J. Wang, C. Xiong, L. Xu, Y. Wang, Y. Wang, Femtosecond laser 3D printed micro objective lens for ultrathin fiber endoscope, Fundamental Research (2022).
[2] Z.Y. Hu, Y.L. Zhang, C. Pan, J.Y. Dou, Z.Z. Li, Z.N. Tian, J.W. Mao, Q.D. Chen, H. B. Sun, Miniature optoelectronic compound eye camera, Nat. Commun. 13 (2022) 5634.
[3] L. Li, A.Y. Yi, Design and fabrication of a freeform microlens array for a compact large-field-of-view compound-eye camera, Appl. Opt. 51 (12) (2012) 1843–1852.
[4] G. E. Davis, J. W. Roblee, and A. R. Hedges, “Comparison of freeform manufacturing techniques in the production of monolithic lens arrays,” in Optical Manufacturing and Testing VIII (SPIE, 2009), 7426, pp. 38–45.
[5] J.Y. Kim, N.B. Brauer, V. Fakhfouri, D.L. Boiko, E. Charbon, G. Grutzner, J. Brugger, Hybrid polymer microlens arrays with high numerical apertures fabricated using simple ink-jet printing technique, Opt. Mater. Express, 1 (2) (2011) 259–269.
[6] J. Fischer, M. Wegener, Three-dimensional optical laser lithography beyond the diffraction limit, Laser Photonics Rev. 7 (1) (2013) 22–44.
[7] B. Wang, Q. Zhang, M. Gu, M. Gu, Aspherical microlenses enabled by two-photon direct laser writing for fiber-optical microendoscopy, Opt. Mater. Express, 10 (2020) 3174–3184.
[8] S. Bianchi, V.P. Rajamanickam, L. Ferrara, E. Di Fabrizio, C. Liberale, R. Di Leonardo, Focusing and imaging with increased numerical apertures through multimode fibers with micro-fabricated optics, Opt. Lett. 38 (2013) 4935–4938.
[9] G. Cojoc, C. Liberale, P. Candeloro, F. Gentile, G. Das, F. De Angelis, E. Di Fabrizio, Optical micro-structures fabricated on top of optical fibers by means of two-photon photopolymerization, Microelectron. Eng. 87 (5-8) (2010) 876–879.
[10] T. Gissibl, S. Thiele, A. Herkommer, H. Giessen, Sub-micrometre accurate free-form optics by three-dimensional printing on single-mode fibres, Nat. Commun. 7 (2016) 11763.
[11] T. Gissibl, M. Schmid, H. Giessen, Spatial beam intensity shaping using phase masks on single-mode optical fibers fabricated by femtosecond direct laser writing, Optica, 3 (4) (2016) 448–451.
[12] S. Schmidt, S. Thiele, A. Toulouse, C. Bösel, T. Tiess, A. Herkommer, H. Gross, H. Giessen, Tailored micro-optical freeform holograms for integrated complex beam shaping, Optica, 7 (10) (2020) 1279–1286.
[13] S. Thiele, K. Arzenbacher, T. Gissibl, H. Giessen, A.M. Herkommer, 3D-printed eagle eye: Compound microlens system for foveated imaging, Sci. Adv. 3 (2017) e1602655.

[14] S. Thiele, T. Gissibl, H. Giessen, A.M. Herkommer, Ultra-compact on-chip LED collimation optics by 3D femtosecond direct laser writing, Opt. Lett., OL 41 (13) (2016) 3029–3032.
[15] Z.N. Tian, X.W. Cao, W.G. Yao, P.X. Li, Y.H. Yu, G. Li, Q.D. Chen, H.B. Sun, Hybrid refractive-diffractive optical vortex microlens, IEEE Photon. Technol. Lett. 28 (21) (2016) 2299–2302.
[16] S. Wong, M. Deubel, F. Pérez-Willard, S. John, G.A. Ozin, M. Wegener, G. von Freymann, Direct laser writing of three- dimensional photonic crystals with a complete photonic bandgap in chalcogenide glasses, Adv. Mater. 18 (3) (2006) 265–269.
[17] T. Gissibl, S. Thiele, A. Herkommer, H. Giessen, Two-photon direct laser writing of ultracompact multi-lens objectives, Nature Photon. 10 (8) (2016) 554–560.
[18] J. Li, S. Thiele, B.C. Quirk, R.W. Kirk, J.W. Verjans, E. Akers, C.A. Bursill, S. J. Nicholls, A.M. Herkommer, H. Giessen, R.A. McLaughlin, Ultrathin monolithic 3D printed optical coherence tomography endoscopy for preclinical and clinical use, Light Sci. Appl. 9 (2020) 124.
[19] J. Li, S. Thiele, R.W. Kirk, B.C. Quirk, A. Hoogendoorn, Y.C. Chen, K. Peter, S. J. Nicholls, J.W. Verjans, P.J. Psaltis, C. Bursill, A.M. Herkommer, H. Giessen, R. A. McLaughlin, 3D-printed micro lens-in-lens for in vivo multimodal microendoscopy, Small, 18 (17) (2022) 2107032.
[20] H. Kim, H. Pyo, H. Kim, and H. W. Kang, "Micro-lens arrays (MLA)-assisted fractional photothermal therapy for effective cancer treatment," in Translational Biophotonics: Diagnostics and Therapeutics (SPIE, 2021), 11919, pp. 4–6.
[21] M. L. Ling, G. S. Chua, Q. Lin, C. J. Tay, and C. Quan, "Customized illumination shapes for 193nm immersion lithography," in Optical Microlithography XXI (SPIE, 2008), 6924, pp. 1066–1076.
[22] X. Xu, K. Kim, W. Jhe, N. Kwon, Efficient optical guiding of trapped cold atoms by a hollow laser beam, Phys. Rev. A 63 (2001) 063401.
[23] L. Paterson, M.P. MacDonald, J. Arlt, W. Sibbett, P.E. Bryant, K. Dholakia, Controlled rotation of optically trapped microscopic particles, Science 292 (2001) 912–914.
[24] S. A. Lerner and B. Dahlgrenn, "Etendue and optical system design," in Nonimaging Optics and Efficient Illumination Systems III (SPIE, 2006), 6338, p. 633801.
[25] A. M. Herkommer, "Evolution of illumination systems in microlithography: a retrospective," in International Optical Design Conference 2010 (SPIE, 2010), 7652, pp. 320–325.
[26] M. Schmid, S. Thiele, A. Herkommer, H. Giessen, Three-dimensional direct laser written achromatic axicons and multi-component microlenses, Opt. Lett. 43 (2018) 5837–5840.